Journal of Quantitative Spectroscopy & Radiative Transfer 276 (2021) 107925

Contents lists available at ScienceDirect

Journal of Quantitative Spectroscopy & Radiative Transfer

journal homepage: www.elsevier.com/locate/jqsrt

Generalization of the complete data fusion to multi-target retrieval of atmospheric parameters and application to FORUM and IASI-NG simulated measurements

Cecilia Tirelli*, Simone Ceccherini, Nicola Zoppetti, Samuele Del Bianco, Ugo Cortesi

Istituto di Fisica Applicata "Nello Carrara" del Consiglio Nazionale delle Ricerche, Via Madonna del Piano 10, Sesto Fiorentino, 50019, Firenze, Italy

A R T I C L E I N F O

Article history:
Received 26 January 2021
Revised 2 September 2021
Accepted 2 September 2021
Available online 4 September 2021

Keywords:
Data fusion
Multi-target retrieval
Synergistic retrieval
Temperature
Water vapour
Ozone

A B S T R A C T

In the context of a growing need for innovatory techniques to take advantage of the largest amount of information from the great number of available remote sensing data, the Complete Data Fusion (CDF) algorithm was presented as a new method to combine independent measurements of the same vertical profile of an atmospheric parameter into a single estimate for a concise and complete characterization of the atmospheric state. The majority of the atmospheric composition measurements determine the altitude distribution of a great number of quantities: multi-target retrievals (MTRs) are increasingly applied to remote sensing observations to determine simultaneously atmospheric constituents with the purpose to reduce the systematic error caused by interfering species. In this work, we optimised the CDF for the application to MTR products. We applied the method to simulated retrievals in the thermal infrared and in the far infrared spectral ranges, considering the instrumental specifications and performances of IASI-NG (Infrared Atmospheric Sounding Interferometer New Generation) and FORUM (Far-Infrared Outgoing Radiation Understanding and Monitoring) instruments, respectively. The obtained results show that the CDF algorithm can cope with state vectors from MTRs, that must share at least one retrieved variable. In particular, the results show that the fused profile has the greatest number of degrees of freedom and the smallest error for all considered cases. The comparison between the CDF products and the synergistic retrieval ones shows the equivalence of the two methods when the linear approximation is adopted to simplify the treatment of the retrieval problem.

1. Introduction

Continuously monitoring the atmosphere over the globe through a great number of satellite missions, as well as airborne and ground-based campaigns is essential to understand processes that control the distribution of atmospheric species and to ensure accurate measurements of their vertical profiles and tridimensional distributions. Moreover, these measurements are important as input in the physical and chemical models used to predict the evolution of the atmospheric state and can be used as source of information in the assimilation systems [1]. In the last few decades, satellite observations have proven their capability to measure a considerable number of atmospheric species [2–6]. In recent years the availability of a large amount of data has stimulated the use of synergistic approaches to gain the largest amount of information from these measurements [7–12].

A synergistic process is based on the combination of a set of satellite observations to obtain products with an enhanced accuracy and information content than the best individual retrieval in the set, exploiting all the possible interactions between the various information inputs. Various approaches, based on different mechanisms, are used to combine multiple sets of independent retrievals of the same atmospheric target [13]. However, two classes of strategies are widely used to determine the vertical profile of atmospheric variables when two or more instruments observe the same portion of atmosphere: the synergistic retrieval and the a posteriori combination of the retrieved products [7].

The synergistic retrieval rigorously combines the redundant and complementary information of different spectral radiance measurements and provides the best estimate of the profile taking into account all the interactions of the different inputs [14]. The implementation of this method is, however, a complex and costly pro-

* Corresponding author.
E-mail address: c.tirelli@ifac.cnr.it (C. Tirelli).

https://doi.org/10.1016/j.jqsrt.2021.107925

cess as it requires a forward radiative transfer model that can deal with a large amount of spectral data and that is suitable to simulate measurements from instruments operating in different spectral ranges. A posteriori combination methods, such as the data fusion, are often used to overcome these difficulties as they propose a different approach [15,16]. In the data fusion approach an algorithm combines, a posteriori, into a single estimate the profiles retrieved independently from spectral measurements of different instruments.

The Complete Data Fusion (CDF) method is based on the a posteriori approach and is able to reduce the complexity of managing high volumes of data and to improve their quality with respect to the operational outcome of individual instruments [17–19]. In particular, the fused products show a higher number of degrees of freedom (DOFs) and an enhanced vertical sensitivity. Moreover, Ceccherini et al. [14] demonstrated in the linear approximation the CDF provides the same solution as the synergistic retrieval with equal error estimates and number of DOFs. It should be remarked that in real problems the linear approximation is not always valid. The value of the CDF procedure is that it uses standard retrieval products obtained with the optimal estimation technique and has very simple implementation requirements, consequently it can be used in remote sensing problems where the application of the synergistic retrieval is too difficult or potentially not possible.

The application of the CDF algorithm, in its current formulation, is limited to retrieval products of a single atmospheric variable. However, multi-target retrievals (MTRs) are increasingly applied to retrieve simultaneously multiple atmospheric constituents from remote sensing observations, thus reducing the systematic error introduced by the interfering species [20–23]. Moreover, MTR allows the use of spectral ranges containing significant contributions from multiple absorbers, which would normally be excluded when each species is retrieved independently. The generalization of the CDF algorithm to fuse profiles obtained from MTRs was a significant step in order to extend its application to remote sensing data that are able to provide high quality products for multiple atmospheric variables.

In this study we simulated synthetic MTR products for the two future satellite missions IASI-NG and FORUM considering two different cases: when their retrieved state vectors coincide completely and when they share only one parameter.

The Infrared Atmospheric Sounding Interferometer - New Generation (IASI-NG) is designed with a very high level of accuracy and it will be dedicated to the characterization of atmospheric composition related to climate, atmospheric chemistry and environment, as well as to operational meteorology and climate monitoring. The objective is to halve the spectral resolution and the radiometric noise in comparison with IASI first generation, assuring an improved performance. The hyper-spectral infrared observation with IASI has been demonstrated to enable an accurate measurement of key gases and atmospheric variables (i.e., carbon monoxide (CO), carbon dioxide (CO_2), water vapour (H_2O), ozone (O_3), sulphur dioxide (SO_2), methane (CH_4)) for climate and atmospheric chemistry monitoring in near real time [24,25]. The second generation of IASI is expected to further improve the quality of these products [26,27].

The Far-infrared Outgoing Radiation Understanding and Monitoring (FORUM) mission will fill the long-standing gap in far-infrared spectral observations and will provide new insight into the planets radiation budget and how it is controlled. Flying in loose formation with the Meteorological Operational Satellite Second Generation (Metop-SG), it will complement mid-infrared spectral measurements by IASI-NG. The main product of the FORUM mission will be the calibrated spectral radiance, however the radiances will be processed up to Level 2 to retrieve atmospheric parameters (in particular water vapour), surface spectral emissivity and cloud parameters in case of cloudy atmospheres. The synergistic use of FORUM and IASI-NG will provide spectrally resolved data of the entire spectrum of the Earth thermal emission with a very high accuracy, improving the monitoring of atmospheric parameters.

This paper presents the feasibility of the CDF with the MTRs products. The simulated FORUM and IASI-NG retrieved profiles are exactly co-located in space and time (they refer to the same atmospheric profile) and are defined on the same vertical grid. The same a priori profile is considered for the simulated retrievals. We simulated the retrieval products adopting the linear approximation in both experiments. These assumptions were made to simplify the problem and were adopted to demonstrate the feasibility of the process in its first step. Following studies will focus on the extension to cases considering inconsistencies in temporal and spatial collocations of multiple instrumental measurements.

The paper is structured as follows. In Section 2, we describe the CDF algorithm and its generalization to MTR. Section 3, we summarize the characteristics and specifications of the instruments. In Section 4, we illustrate the generation of the synthetic data of IASI-NG and FORUM. In Section 5, we show the results obtained with the application of the CDF to the simulated MTR products. Finally, in Section 6, we summarize the results of the work and draw the conclusions.

2. The CDF method

2.1. CDF equations

The CDF [14] is a data fusion method that takes into account the main features of the measurements to be combined. For its formulation it could be seen an extension of the weighted mean to the case in which the averaging kernel matrices (AKMs) are different from the identity matrix. The CDF algorithm is applied when N vertical profiles of atmospheric variables are retrieved, using the optimal estimation method [28], from N simultaneous and independent measurements. The retrieved profiles (fusing profiles) are characterized by their state vectors $\hat{\mathbf{x}}_i$ (i=1, 2, N), their retrieval noise error covariance matrices (CMs) $\mathbf{S}_i$, their AKMs $\mathbf{A}_i$ [28–30] and are used in input to the following equations to obtain the CDF solution $\mathbf{x}_f$. This solution depends on the N input quantities ($\hat{\mathbf{x}}_i$, $\mathbf{A}_i$, $\mathbf{S}_i$), on the a priori profile $\hat{\mathbf{x}}_a$ and the covariance matrix of the a priori $\mathbf{S}_a$ used to constrain the fused product. It is given by:

$$\mathbf{x}_f = \left(\sum_{i=1}^{N} \mathbf{A}_i^T \mathbf{S}_i^{-1} \mathbf{A}_i + \mathbf{S}_a^{-1}\right)^{-1} \left(\sum_{i=1}^{N} \mathbf{A}_i^T \mathbf{S}_i^{-1} \boldsymbol{\alpha}_i + \mathbf{S}_a^{-1} \mathbf{x}_a\right), \quad (1)$$

where

$$\boldsymbol{\alpha}_i \equiv \hat{\mathbf{x}}_i - (\mathbf{I} - \mathbf{A}_i)\mathbf{x}_{ai}, \quad (2)$$

$\mathbf{I}$ is the identity matrix and $\mathbf{x}_{ai}$ is the a priori profile for the individual retrieval. In this study the a priori profiles and CMs are the same for the individual retrievals of IASI-NG and FORUM and for the fused product. The use of the same a priori information in all products allows to easily compare the performance of the two individual measurements with respect to the fusion.

The error CM and AKM of the fused profile are given by:

$$\mathbf{S}_f = \left(\sum_{i=1}^{N} \mathbf{A}_i^T \mathbf{S}_i^{-1} \mathbf{A}_i + \mathbf{S}_a^{-1}\right)^{-1} \sum_{i=1}^{N} \mathbf{A}_i^T \mathbf{S}_i^{-1} \mathbf{A}_i \left(\sum_{i=1}^{N} \mathbf{A}_i^T \mathbf{S}_i^{-1} \mathbf{A}_i + \mathbf{S}_a^{-1}\right)^{-1} \quad (3)$$

$$\mathbf{A}_f = \left(\sum_{i=1}^{N} \mathbf{A}_i^T \mathbf{S}_i^{-1} \mathbf{A}_i + \mathbf{S}_a^{-1}\right)^{-1} \sum_{i=1}^{N} \mathbf{A}_i^T \mathbf{S}_i^{-1} \mathbf{A}_i \quad (4)$$

The fusing profiles are, in general, not exactly collocated in space and time and defined on different retrieval grids. The application of the CDF method to vertical profiles observing different true profiles and obtained with different instruments on different retrieval grids was analyzed in Ceccherini et al. [17] for the CDF application to single parameter state vectors. Additional sources of errors and their corresponding CMs should be introduced when the vertical fusion grid does not coincide with the grids of the fusing profiles (interpolation error) and when their space and time locations are not coincident (coincidence error) [31]. In this work, such errors are not considered as the simulated fusing profiles are defined on the same vertical grid of the fused profile and are referred to the same true profile. This is an approximation that simplifies the real processing of multi-sensor data and that we adopted as the first step of the process that aims to reproduce, as final result, the real case. As in the case of single parameters state vectors, further applications will consider coincidence and interpolation errors to be applied to fusing profiles from MTRs.

2.2. Generalization of the CDF method to MTR

In this section, we describe the generalization of the CDF method for its application with input vectors and matrices ($\hat{\mathbf{x}}_i$, $\mathbf{S}_i$, $\mathbf{A}_i$) from MTRs. Suppose to retrieve N state vectors $\hat{\mathbf{x}}_i$(i=1,...,N) with M_i parameters from the spectral measurements vectors $\mathbf{y}_i$. The N state vectors $\hat{\mathbf{x}}_i$ may have one or more of the M_i parameters in common. The following equations are valid in the case in which the N vectors have the same number of parameters M_i. The MTR outputs obtained with the optimal estimation can be written as:

$$\hat{\mathbf{x}}_i = \begin{pmatrix} \mathbf{P1}_i \\ \mathbf{P2}_i \\ \mathbf{P3}_i \\ . \\ . \\ . \\ \mathbf{PM}_i \end{pmatrix} \mathbf{A}_i = \begin{pmatrix} \mathbf{A_{11}}_{,i} & \mathbf{A_{12}}_{,i} & . & . & . & \mathbf{A_{1M}}_{,i} \\ \mathbf{A_{21}}_{,i} & \mathbf{A_{22}}_{,i} & . & . & . & \mathbf{A_{2M}}_{,i} \\ . & . & . & . & . & . \\ . & . & . & . & . & . \\ \mathbf{A_{M1}}_{,i} & \mathbf{A_{M2}}_{,i} & . & . & . & \mathbf{A_{MM}}_{,i} \end{pmatrix}$$
$$\mathbf{S}_i = \begin{pmatrix} \mathbf{S_{11}}_{,i} & \mathbf{S_{12}}_{,i} & . & . & . & \mathbf{S_{1M}}_{,i} \\ \mathbf{S_{21}}_{,i} & \mathbf{S_{22}}_{,i} & . & . & . & \mathbf{S_{2M}}_{,i} \\ . & . & . & . & . & . \\ . & . & . & . & . & . \\ \mathbf{S_{M1}}_{,i} & \mathbf{S_{M2}}_{,i} & . & . & . & \mathbf{S_{MM}}_{,i} \end{pmatrix} \quad (5)$$

where $\mathbf{Pk}_i$ (k=1,...,M) is a subvector corresponding to the kth parameter (e.g temperature, water vapour and ozone). For readability in the following equations we omit the i subscript. $\mathbf{A_{rq}}$ and $\mathbf{S_{rq}}$ are submatrices defined as:

$$\mathbf{A}_{rq} = \frac{\partial \hat{\mathbf{Pr}}}{\partial \mathbf{Pq}} \quad (6)$$

and

$$\mathbf{S}_{rq} = \left\langle (\hat{\mathbf{Pr}} - \langle \hat{\mathbf{Pr}} \rangle)(\hat{\mathbf{Pq}} - \langle \hat{\mathbf{Pq}} \rangle)^T \right\rangle \quad (7)$$

where $\hat{\mathbf{Pk}}$ is the retrieved value, $\mathbf{Pk}$ is the true value and $\langle\rangle$ denotes the expected value of the quantity (see Eq. 2.10 of [28]). The subscripts $\boldsymbol{r}$ and $\boldsymbol{q}$ (where $\boldsymbol{r}$, $\boldsymbol{q}$= 1,...,M) refer to the k parameters.

2.2.1. MTR with the same retrieved parameters

If the fusing measurements are MTR state vectors that contain the same atmospheric variables we can use the standard CDF equations (Eq. (1), (3), (4)). To simplify the description we consider the case of two measurements whose state vectors contain the same two parameters: $\hat{\mathbf{x}}_1 = \begin{pmatrix} \mathbf{P1}_1 \\ \mathbf{P2}_1 \end{pmatrix}$ and $\hat{\mathbf{x}}_2 = \begin{pmatrix} \mathbf{P1}_2 \\ \mathbf{P2}_2 \end{pmatrix}$. The state vectors $\hat{\mathbf{x}}_1$ and $\hat{\mathbf{x}}_2$ with the corresponding AKMs $\mathbf{A}_1$, $\mathbf{A}_2$ and CMs $\mathbf{S}_1$, $\mathbf{S}_2$ to be used in input to the MTR CDF are:

$$\hat{\mathbf{x}}_i = \begin{pmatrix} \mathbf{P1}_i \\ \mathbf{P2}_i \end{pmatrix} \mathbf{A}_i = \begin{pmatrix} \mathbf{A_{11}}_{,i} & \mathbf{A_{12}}_{,i} \\ \mathbf{A_{21}}_{,i} & \mathbf{A_{22}}_{,i} \end{pmatrix} \mathbf{S}_i = \begin{pmatrix} \mathbf{S_{11}}_{,i} & \mathbf{S_{12}}_{,i} \\ \mathbf{S_{21}}_{,i} & \mathbf{S_{22}}_{,i} \end{pmatrix} \quad (8)$$

with i=1,2. $\mathbf{Pk}_i$, $\mathbf{A_{rq}}_i$, $\mathbf{S_{rq}}_i$ are sub-vectors and sub-matrices of the input state vectors, AKMs and CMs referring to the corresponding parameters as defined in Eqs. (6) and (7). Using these matrices as input to the MTR CDF algorithm, we obtain this solution:

$$\hat{\mathbf{x}}_f = \begin{pmatrix} \mathbf{P1}_f \\ \mathbf{P2}_f \end{pmatrix} \mathbf{A}_f = \begin{pmatrix} \mathbf{A_{11}}_{,f} & \mathbf{A_{12}}_{,f} \\ \mathbf{A_{21}}_{,f} & \mathbf{A_{22}}_{,f} \end{pmatrix} \mathbf{S}_f = \begin{pmatrix} \mathbf{S_{11}}_{,f} & \mathbf{S_{12}}_{,f} \\ \mathbf{S_{21}}_{,f} & \mathbf{S_{22}}_{,f} \end{pmatrix} \quad (9)$$

2.2.2. MTR with different retrieved parameters

In addition to (at least) one common parameter, the fusing state vectors might contain different (not in common) atmospheric variables, in that case we need to modify the state vectors and the matrices in input. In order to apply the CDF method the state vectors are modified to be the union of the parameters retrieved from the different measurements and new AKMs and CMs are created, adding sub-matrices related to the non-retrieved parameters and considering that no information is retrieved for them. To simplify the description we consider the case of two measurements with state vectors with one parameter in common and one different parameter each: $\hat{\mathbf{x}}_1 = \begin{pmatrix} \mathbf{P1}_1 \\ \mathbf{P2}_1 \end{pmatrix}$ and $\hat{\mathbf{x}}_2 = \begin{pmatrix} \mathbf{P1}_2 \\ \mathbf{P3}_2 \end{pmatrix}$. The new state vectors $\hat{\mathbf{x}}_1$ and $\hat{\mathbf{x}}_2$ with the corresponding AKMs $\mathbf{A}_1$, $\mathbf{A}_2$ and CMs $\mathbf{S}_1$, $\mathbf{S}_2$ to be used in input to the MTR CDF are:

$$\hat{\mathbf{x}}_1 = \begin{pmatrix} \mathbf{P1}_1 \\ \mathbf{P2}_1 \\ \mathbf{0} \end{pmatrix} \mathbf{A}_1 = \begin{pmatrix} \mathbf{A_{11}}_{,1} & \mathbf{A_{12}}_{,1} & 0 \\ \mathbf{A_{21}}_{,1} & \mathbf{A_{22}}_{,1} & 0 \\ 0 & 0 & 0 \end{pmatrix} \mathbf{S}_1 = \begin{pmatrix} \mathbf{S_{11}}_{,1} & \mathbf{S_{12}}_{,1} & 0 \\ \mathbf{S_{21}}_{,1} & \mathbf{S_{22}}_{,1} & 0 \\ 0 & 0 & 0 \end{pmatrix} \quad (10)$$

$$\hat{\mathbf{x}}_2 = \begin{pmatrix} \mathbf{P1}_2 \\ \mathbf{0} \\ \mathbf{P3}_2 \end{pmatrix} \mathbf{A}_2 = \begin{pmatrix} \mathbf{A_{11}}_{,2} & 0 & \mathbf{A_{13}}_{,2} \\ 0 & 0 & 0 \\ \mathbf{A_{31}}_{,2} & 0 & \mathbf{A_{33}}_{,2} \end{pmatrix} \mathbf{S}_2 = \begin{pmatrix} \mathbf{S_{11}}_{,2} & 0 & \mathbf{S_{13}}_{,2} \\ 0 & 0 & 0 \\ \mathbf{S_{31}}_{,2} & 0 & \mathbf{S_{33}}_{,2} \end{pmatrix}. \quad (11)$$

The retrieval noise CM has zero elements for the not retrieved parameter as no information comes from the retrieval, thus the component of the measurement error for that parameter does not propagate (see Par.5.4.2 of [28]). The error CM of Eqs. (9) and (11), having diagonal elements equal to zero, are not invertible. Thus, for the inversion of the error CM in the CDF solution equations (Eq. (1), (3), (4)) we calculated the generalized inverse [32]. $\mathbf{Pk}_i$, $\mathbf{A_{rq}}_i$, $\mathbf{S_{rq}}_i$ are sub-vectors and sub-matrices of the input state vectors, CMs and AKMs referring to the corresponding parameters as defined in Eqs. (6) and (7). Using the new matrices as input to the MTR CDF algorithm, we obtain a solution that contains elements in common and not in common:

$$\hat{\mathbf{x}}_f = \begin{pmatrix} \mathbf{P1}_f \\ \mathbf{P2}_f \\ \mathbf{P3}_f \end{pmatrix} \mathbf{A}_f = \begin{pmatrix} \mathbf{A_{11}}_{,f} & \mathbf{A_{12}}_{,f} & \mathbf{A_{13}}_{,f} \\ \mathbf{A_{21}}_{,f} & \mathbf{A_{22}}_{,f} & \mathbf{A_{23}}_{,f} \\ \mathbf{A_{31}}_{,f} & \mathbf{A_{32}}_{,f} & \mathbf{A_{33}}_{,f} \end{pmatrix} \mathbf{S}_f = \begin{pmatrix} \mathbf{S_{11}}_{,f} & \mathbf{S_{12}}_{,f} & \mathbf{S_{13}}_{,f} \\ \mathbf{S_{21}}_{,f} & \mathbf{S_{22}}_{,f} & \mathbf{S_{23}}_{,f} \\ \mathbf{S_{31}}_{,f} & \mathbf{S_{32}}_{,f} & \mathbf{S_{33}}_{,f} \end{pmatrix} \quad (12)$$

3. Instruments

The Infrared Atmospheric Sounding Interferometer - New Generation (IASI-NG) will be one of the main instruments onboard the second generation of European Meteorological Operational satellites (MetOp-SG) that will guarantee the continuation of meteorological observations from polar orbit in the expected 2022–2043 time frame. The orbit average altitude of MetOp-SG-1A satellite will be 830 km and its inclination will be 98.7 degrees with a mean local solar time of 09:30 at the descending node. The repeat cycle will be of 29 days and it will consist of 412 orbits.

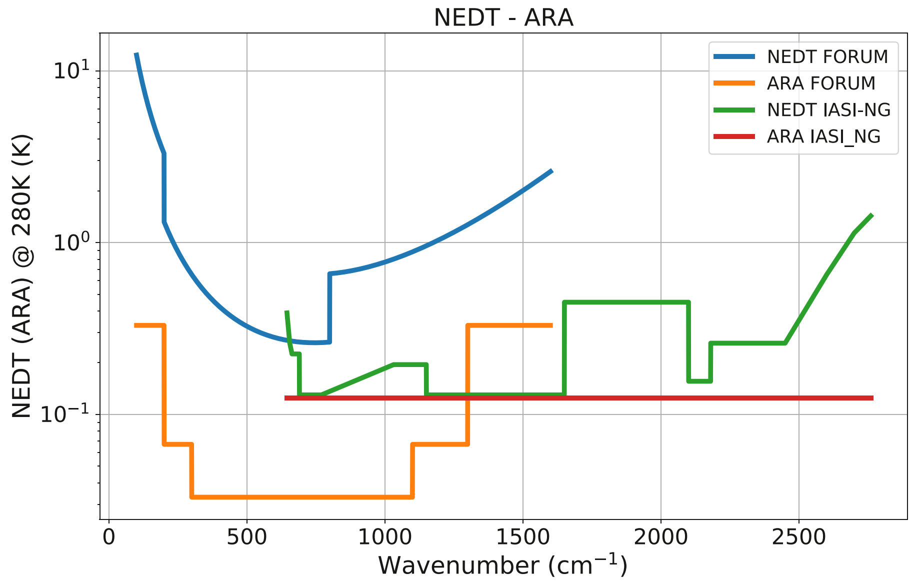

Fig. 1. Summary of NEDT and ARA for IASI-NG and FORUM. For comparability, errors are shown as 1 sigma bounds.

Table 1
Summary of IASI-NG and FORUM main characteristics.

	Instrument	
Characteristic	IASI-NG	FORUM
Spectral Coverage	645 - 2760 cm^{-1}	100 - 1600 cm^{-1}
Spectral Resolution	0.25 cm^{-1}	0.5 cm^{-1}
Spectral Sampling	0.125 cm^{-1}	0.413 cm^{-1}
Measurement mode	step and stare (azimuth scanning)	step and stare (no azimuth scanning)
Ground pixel (diameter at nadir)	12 km	15 km

The IASI-NG [26] instrument is a Fourier Transform Spectrometer that will measure the Mid-Infrared (MIR) radiation (from 645 to 2760 cm^{-1}) emitted by the Earth with a spectral resolution after apodization of 0.25 cm^{-1}, a spectral sampling of 0.125 cm^{-1} and a reduced radiometric noise with respect to its predecessor IASI (at least of a factor of 2, see Fig. 1 of [26]). IASI-NG will scan across the track in a step and scare mode with 7 Field of Regards (FORs) placed symmetrically by either side of the nadir for each scan cycle. Each FOR contains a 4×4 system of Fields of View (FOVs), assuring a total of 14×16 FOVs each scan line. The diameter at nadir of the ground pixel is 12 km.

The Far-infrared Outgoing Radiation Understanding and Monitoring (FORUM) [33] will be the ninth Earth Explorer mission of the European Space Agency and its launch, on board a polar orbiting satellite, is scheduled in 2025–2026. The orbit characteristics of the sun-synchronous polar orbiting satellite, hosting the FORUM mission instrument, will be the same of MetOp-SG-1A satellite, hosting IASI-NG. The main instrument of the FORUM mission will be a Fourier Transform Spectrometer that will measure the Far-Infrared (FIR) and MIR portion of the spectrum (from 100 to 1600 cm^{-1}) emitted by the Earth. The unapodized spectral resolution of the calibrated spectral radiances is 0.5 cm^{-1} and the spectral sampling step is 0.413 cm^{-1}. FORUM will measure in a step and stare mode: it will observe a fixed circular ground pixel of 15 km diameter for the whole time interval of the measurement, without azimuth scanning. We simulated the IASI-NG and FORUM products considering the most recent instrumental specification, resumed in Table 1 [26,33–35].

Fig. 1 summarizes the assumed FORUM and IASI-NG Noise Equivalent Delta Temperature (NEDT) and Absolute Radiometric Accuracy (ARA) error specifications: a black body source at 280 K is assumed and all values have been scaled to 1 sigma for an easier comparison.

IASI-NG and FORUM will fly in loose formation (i.e, the time lag between FORUM and MetOp-SG-1A shall be less than 1 min and the maximum distance between ground tracks of the two satellite orbits shall be less than 100 km as a goal). In accordance with the measurements geometries and orbits characteristics, as well as with the requirements for the loose-formation, the FORUM pixel and the nearest IASI-NG sub-satellite centre will be separated by less than 23 km [33]. For an illustration of IASI-NG and FORUM patterns see Fig. 3 of [33]. For their characteristics, IASI-NG and FORUM matching measurements are suitable for a synergistic exploitation, offering the opportunity to generate improved Level 2 products.

4. Simulated measurements

Simulations of IASI-NG and FORUM MTR retrieval products were carried out using the KLIMA (Kyoto protocoL Informed Management of the Adaptation) forward and retrieval model described in [36] and references contained therein. We adapted the KLIMA code to simulate the retrieved synthetic products with the algorithm described in the following Section 4.1. The formalism of Section 4.1 was used to simulate profiles, error CMs and AKMs in the following spectral ranges: 645–770 cm^{-1} and 1030–1400 cm^{-1} for IASI-NG and 100–1600 cm^{-1} for FORUM. The spectral range selection for IASI-NG was made to optimize the retrieval performances [16,26,37–39] and to reduce the computational time.

Three clear-sky atmospheric scenarios were selected from MERRA2 (Modern-Era Retrospective analysis for Research and Ap-

Table 2
Scheme for the experiments description: the retrieved parameters are shown for each experiment and each instrument or data combination approach (CDF and synergistic retrieval).

	Experiment 1	Experiment 2
IASI-NG	Temperature - H_2O	Temperature - O_3
FORUM	Temperature - H_2O	Temperature - H_2O
FUSED	Temperature - H_2O	Temperature - H_2O - O_3
SYNERGISTIC	Temperature - H_2O	-

plications, Version 2) [40] reanalysis in order to consider a variety of atmospheric conditions for this study:

- SCENARIO 1 (hereafter TROPICS): lat: -18.96, lon: 131.55; date: 1 April 2012 (daytime); surface: water.
- SCENARIO 2 (hereafter MIDLAT): lat: 49.71, lon: 11.08; date: 2 April 2012 (daytime); surface: water.
- SCENARIO 3 (hereafter POLAR): lat: 74.38, lon: -169.64; date: 2 April 2012 (daytime); surface: water.

Each scenario defines the state of the atmosphere, providing information on temperature, water-vapour, ozone, cloud coverage. The database contains: geolocation, date, temperature, surface temperature, surface pressure, surface emissivity and land/sea classification. The selected scenarios are not characterized by thermal inversion. Vertical profiles of 30 trace gases were taken from the Initial Guess for Level 2 (IG2) climatological database [41]

The a priori profiles and a priori CMs were extracted from the MARS (Meteorological Archival and Retrieval System) archive of the European Centre for Medium-Range Weather Forecasts (ECMWF) [42,43]. The simulated FORUM spectral radiance reaching the instrument was convolved by the ISRF (Instrumental Spectral Response Function), defined as a *sinc* function with a distance of 0.413 cm^{-1} between the main maximum and the first adjacent zero (FWHM=0.5 cm^{-1}), and the spectrum was apodized with the Norton-Beer strong function. Finally a random noise with an amplitude of the order of the NESR was added. IASI-NG data have been simulated considering that measurements will provide a spectrum apodized with a Gaussian function with a Full Width at Half Maximum (FWHM) coinciding with the spectral resolution (0.25 cm^{-1}), and that the spectral sampling step will be of 0.125 cm^{-1}.

We carried out two experiments (see Table 2): in the first one we simulated the MTR of temperature and water-vapour profiles for IASI-NG and FORUM, in the second one of temperature and water-vapour profiles for FORUM and temperature and ozone profiles for IASI-NG. In the first experiment we also simulated the synergistic retrieval of IASI-NG and FORUM for the MTR of temperature and water vapour profiles for a comparison with the data fusion results. The temperature profiles and the gas volume mixing ratios (vmr) are simulated considering a retrieval on a vertical grid at fixed pressure levels from 0 to 65 km with a step of about 2 km.

4.1. Simulation algorithm

4.1.1. IASI-NG and FORUM L2 products

The simulation of the Level 2 products (i.e the geophysical products retrieved from the measured radiances) of IASI-NG and FORUM is based on the optimal estimation theory [28]. In the two experiments, the retrieved states of IASI-NG (I) and FORUM (F) have been calculated as [44]:

$$\hat{\mathbf{x}}_i = \mathbf{A}_i\mathbf{x}_{true} + (\mathbf{I} - \mathbf{A}_i)\mathbf{x}_a + \delta_i \tag{13}$$

where i=I,F. In Eq. (13) $\mathbf{A}_i$ is the AKM, $\mathbf{x}_{true}$ is the true profile provided by the atmospheric scenario, $\mathbf{x}_a$ is the a priori profile provided by the MARS climatology and δ_i is the retrieval error. The AKM $\mathbf{A}_i$ has been computed as:

$$\mathbf{A}_i = \left(\mathbf{K}_i^T\mathbf{S_y}_i^{-1}\mathbf{K}_i + \mathbf{S}_a^{-1}\right)^{-1}\mathbf{K}_i^T\mathbf{S_y}_i^{-1}\mathbf{K}_i \tag{14}$$

where $\mathbf{K_i}$ is the Jacobian matrix of the forward model calculated in $\mathbf{x}_{true}$, $\mathbf{S_y}_i$ is the error CM of the observations and $\mathbf{S}_a$ is the error CM of the a priori profile.

The retrieval error is given by:

$$\delta_i = \mathbf{G}_i\epsilon_i = \left(\mathbf{K}_i^T\mathbf{S_y}_i^{-1}\mathbf{K}_i + \mathbf{S}_a^{-1}\right)^{-1}\mathbf{K}_i^T\mathbf{S_y}_i^{-1}\epsilon_i \tag{15}$$

where $\mathbf{G}_i$ is the gain matrix and ϵ_i in the error on the observations. ϵ_i is randomly taken from a Gaussian distribution with average zero and a CM $\mathbf{S_y}_i$. The CM of the retrieval error δ_i is calculated as:

$$\mathbf{S}_i = \left(\mathbf{K}_i^T\mathbf{S_y}_i^{-1}\mathbf{K}_i + \mathbf{S}_a^{-1}\right)^{-1}\mathbf{K}_i^T\mathbf{S_y}_i^{-1}\mathbf{K}_i\left(\mathbf{K}_i^T\mathbf{S_y}_i^{-1}\mathbf{K}_i + \mathbf{S}_a^{-1}\right)^{-1} \tag{16}$$

Summing the CM of the retrieval noise $\mathbf{S}_i$ with the CM of the smoothing error $\mathbf{S}_{s,i}$:

$$\mathbf{S}_{s,i} = \left(\mathbf{K}_i^T\mathbf{S_y}_i^{-1}\mathbf{K}_i + \mathbf{S}_a^{-1}\right)^{-1}\mathbf{S}_a^{-1}\left(\mathbf{K}_i^T\mathbf{S_y}_i^{-1}\mathbf{K}_i + \mathbf{S}_a^{-1}\right)^{-1} \tag{17}$$

we obtain the CM of the total error:

$$\mathbf{S}_{tot,i} = \mathbf{S}_i + \mathbf{S}_{s,i} = \left(\mathbf{K}_i^T\mathbf{S_y}_i^{-1}\mathbf{K}_i + \mathbf{S}_a^{-1}\right)^{-1} \tag{18}$$

4.1.2. Synergistic products

Since measurements of IASI-NG and FORUM will be indipendent from one another, the AKM of the synergistic product $\mathbf{A}_{syn}$ has been calculated by:

$$\mathbf{A}_{syn} = \left(\mathbf{K}_I^T\mathbf{S_y}_I^{-1}\mathbf{K}_I + \mathbf{K}_F^T\mathbf{S_y}_F^{-1}\mathbf{K}_F + \mathbf{S}_a^{-1}\right)^{-1}\left(\mathbf{K}_I^T\mathbf{S_y}_I^{-1}\mathbf{K}_I + \mathbf{K}_F^T\mathbf{S_y}_F^{-1}\mathbf{K}_F\right) \tag{19}$$

where $\mathbf{K}_I$ and $\mathbf{K}_F$ are the Jacobians of the simulated IASI-NG and FORUM measurements, respectively. $\mathbf{S_y}_I$ and $\mathbf{S_y}_F$ are the CMs representing IASI-NG and FORUM measurement errors and $\mathbf{S}_a$ is the error CM of the a priori state vector. The synergistic retrieval and smoothing error CMs are computed, respectively, as:

$$\mathbf{S}_{syn} = \left(\mathbf{K}_I^T\mathbf{S_y}_I^{-1}\mathbf{K}_I + \mathbf{K}_F^T\mathbf{S_y}_F^{-1}\mathbf{K}_F + \mathbf{S}_a^{-1}\right)^{-1}\left(\mathbf{K}_I^T\mathbf{S_y}_I^{-1}\mathbf{K}_I + \mathbf{K}_F^T\mathbf{S_y}_F^{-1}\mathbf{K}_F\right) \cdot\left(\mathbf{K}_I^T\mathbf{S_y}_I^{-1}\mathbf{K}_I + \mathbf{K}_F^T\mathbf{S_y}_F^{-1}\mathbf{K}_F + \mathbf{S}_a^{-1}\right)^{-1} \tag{20}$$

and:

$$\mathbf{S}_{s,syn} = \left(\mathbf{K}_I^T\mathbf{S_y}_{,I}^{-1}\mathbf{K}_I + \mathbf{K}_F^T\mathbf{S_y}_F^{-1}\mathbf{K}_F + \mathbf{S}_a^{-1}\right)^{-1}\mathbf{S}_a^{-1} \cdot\left(\mathbf{K}_I^T\mathbf{S_y}_I^{-1}\mathbf{K}_I + \mathbf{K}_F^T\mathbf{S_y}_F^{-1}\mathbf{K}_F + \mathbf{S}_a^{-1}\right)^{-1} \tag{21}$$

The CM of the total error for the synergistic product is expressed by:

$$\mathbf{S}_{tot,syn} = \mathbf{S}_{syn} + \mathbf{S}_{s,syn} = \left(\mathbf{K}_I^T\mathbf{S_y}_{,I}^{-1}\mathbf{K}_I + \mathbf{K}_F^T\mathbf{S_y}_{,F}^{-1}\mathbf{K}_F + \mathbf{S}_a^{-1}\right)^{-1} \tag{22}$$

5. Results

In this section, we will show the results for the two experiments described above (Section 2): the CDF algorithm applied to MTR synthetic measurements of IASI-NG and FORUM when the retrieved parameters of fusing measurements coincide completely (experiment 1: MTR with the same retrieved parameters, Section 5.1) and when they share only one parameter (experiment 2: MTR with different retrieved parameters, Section 5.2). For both cases, we will show the analysis of the differences of IASI-NG, FORUM, fused, a priori profiles with the true profile, the number of DOFs and the retrieval information gain for all retrieved and fused profiles. In the first case, when IASI-NG and FORUM measure the same parameters (temperature and H_2O), the difference between the fused profile and the synergistic retrieval is also considered.

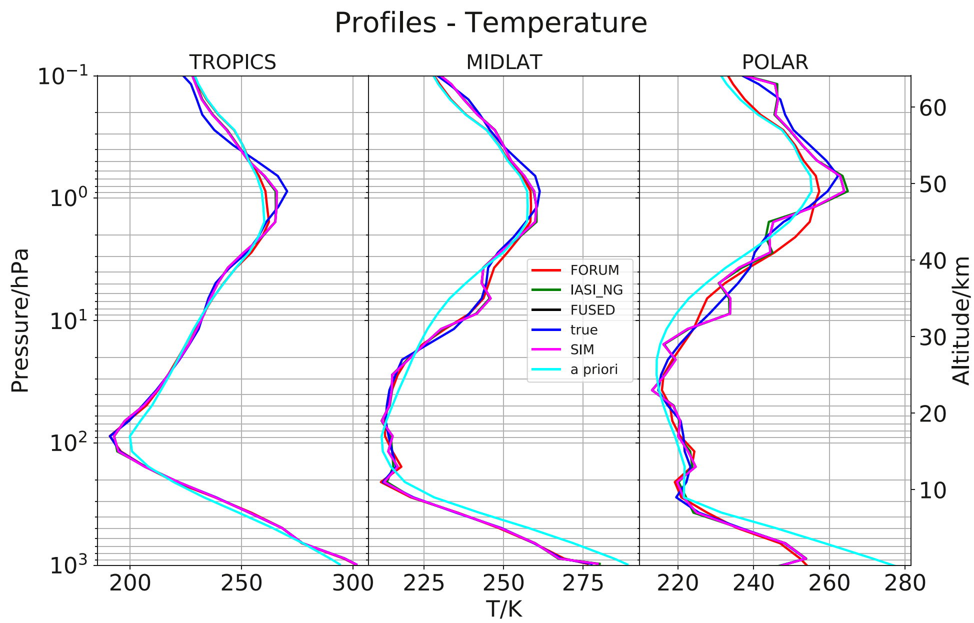

Fig. 2. Temperature profiles for IASI-NG (green line), FORUM (red line), synergistic (magenta line) and fused (black line) products and the corresponding true profile (blue line) in the three atmospheric scenarios: TROPICS (left), MIDLAT (central) and POLAR (right). The a priori profile is also shown (cyan line). The synergistic and fused profiles are completely overlapped, thus it is impossible to distinguish the corresponding curves.

5.1. Experiment 1: MTR with the same retrieved parameters

In this case, the state vectors of IASI-NG (I) and FORUM (F) fusing measurements contain the same atmospheric variables: temperature (T) and water vapour (H_2O). Their state vectors, AKMs and error CMs are defined by the following:

$$\hat{\mathbf{x}}_i = \begin{pmatrix} \mathsf{T}_i \\ \mathsf{H_2O}_i \end{pmatrix} \mathsf{A}_i = \begin{pmatrix} \mathsf{A}_{\mathsf{T},i} & \mathsf{A}_{\mathsf{TH_2O},i} \\ \mathsf{A}_{\mathsf{H_2OT},i} & \mathsf{A}_{\mathsf{H_2O},i} \end{pmatrix} \mathsf{S}_i = \begin{pmatrix} \mathsf{S}_{\mathsf{T},i} & \mathsf{S}_{\mathsf{TH_2O},i} \\ \mathsf{S}_{\mathsf{H_2OT},i} & \mathsf{S}_{\mathsf{H_2O},i} \end{pmatrix} \tag{23}$$

where i=I,F and the CDF solution is given by:

$$\hat{\mathbf{x}}_f = \begin{pmatrix} \mathsf{T}_f \\ \mathsf{H_2O}_f \end{pmatrix} \mathsf{A}_f = \begin{pmatrix} \mathsf{A}_{\mathsf{T},f} & \mathsf{A}_{\mathsf{TH_2O},f} \\ \mathsf{A}_{\mathsf{H_2OT},f} & \mathsf{A}_{\mathsf{H_2O},f} \end{pmatrix} \mathsf{S}_f = \begin{pmatrix} \mathsf{S}_{\mathsf{T},f} & \mathsf{S}_{\mathsf{TH_2O},f} \\ \mathsf{S}_{\mathsf{H_2OT},f} & \mathsf{S}_{\mathsf{H_2O},f} \end{pmatrix} \tag{24}$$

In order to compare the fused (f) and individual measurements with the true profile (as reference) we calculated:

- the absolute difference between IASI-NG, FORUM, fused profiles and the true profile (for both parameters).
- the percentage difference between IASI-NG, FORUM, fused profiles and the true profile (for water vapour, in order to show the behaviour along the entire profile).

We also calculated the absolute and percentage differences between the a priori profile and the true profile for a comprehensive analysis of the results.

As the two input measurements contain the same parameters, we calculated the synergistic retrieval of IASI-NG and FORUM (see Section 4.1.2) and we compared the CDF results with those of the synergistic retrieval to demonstrate the equivalence between the two methods (demonstrated in [14] for single variable retrievals) also in case of MTR. We calculated the absolute and percentage differences considering the synergistic retrieval profile ($\mathbf{x}_s$) as reference for the fused one.

In order to estimate quantitatively the quality improvement of the CDF application with respect to the use of the individual products (both experiments) and of the synergistic retrieval (for experiment 1 only) we calculated:

- the number of Degrees of Freedom (DOFs), a scalar measure of the number of independent quantities that can be measured, given by the trace of the AK matrix [28].
- the Shannon Information Content (SIC), defined as [28]:

$$\Delta I = 0.5 * (\log_2 |\mathsf{S}_a| - \log_2 |\mathsf{S}_{tot,i}|) \tag{25}$$

where $|\mathsf{S}_a|$ and $|\mathsf{S}_{tot,i}|$ are the determinants of the VCMs of the a priori profile and of the retrieved profile. The SIC value provides the information gain obtained with the retrieval process with respect to the information given by the a priori profile.

In Fig. 2 and 3, the temperature and water vapour profiles are shown for the a priori and true profiles and for the two fusing measurements, the fused and the synergistic retrieval profiles. The differences between the profiles' values are more evident in the polar scenario for both parameters and, in general, in the UTLS region for temperature and in the lower troposphere for H_2O. The synergistic and fused profiles are completely overlapped, thus it is impossible to distinguish the corresponding curves.

Figs. 4 and 5 (top) show the absolute differences between IASI-NG, FORUM, fused, a priori profiles and the true profile for temperature and water vapour. The differences between fused and synergistic retrieval profiles are also shown. In order to better visualize the results of the absolute difference for water vapour the y-axis scale is reduced to the range from the ground pressure to a pressure of 100 hPa (from 0 to near 16 km in altitude).

For water vapour also percentage differences (Eq. (15) and (16)) are shown in Fig. 5 (bottom), as explained above. Fig. 4 shows that the absolute differences with the true profile for temperature are less than 5 K, except for the upper stratosphere where they reach values of 10 K for FORUM profile. For H_2O the percentage differences are higher in the troposphere, where they reach values greater than 50%, with peaks exceeeding 100% for the polar scenario. The H_2O concentration in the UTLS and stratosphere is less than 10 ppmv, thus the analysis of the % difference values in this region is less informative. In Figs. 4 and 5, the magenta line behaviour demonstrates that the difference between the

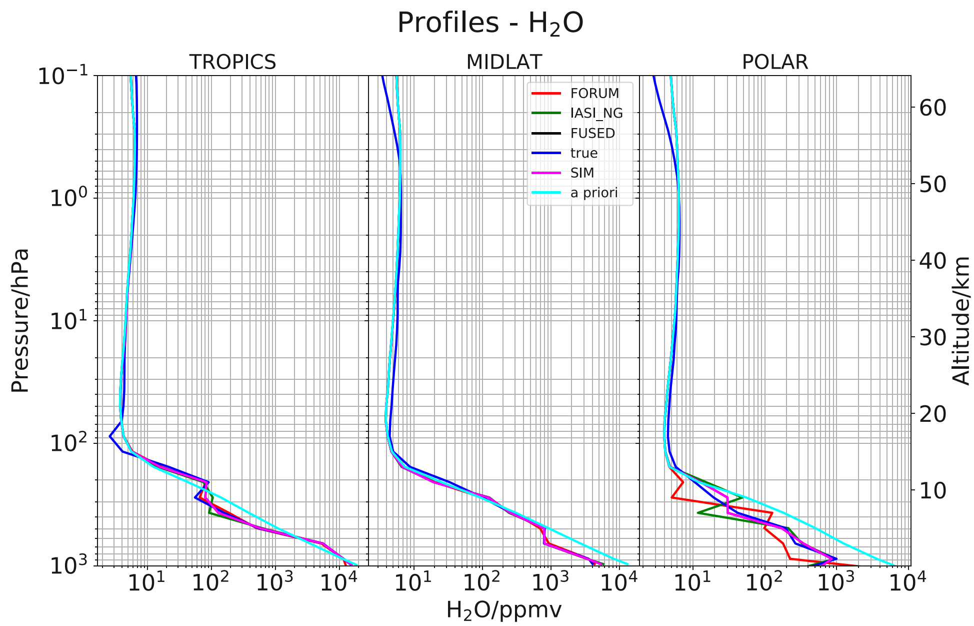

Fig. 3. Water vapour profiles for IASI-NG (green line), FORUM (red line), synergistic (magenta line) and fused (black line) products and the corresponding true profile (blue line) in the three atmospheric scenarios: TROPICS (left), MIDLAT (central) and POLAR (right). The a priori profile is also shown (cyan line). The synergistic and fused profiles are completely overlapped, thus it is impossible to distinguish the corresponding curves.

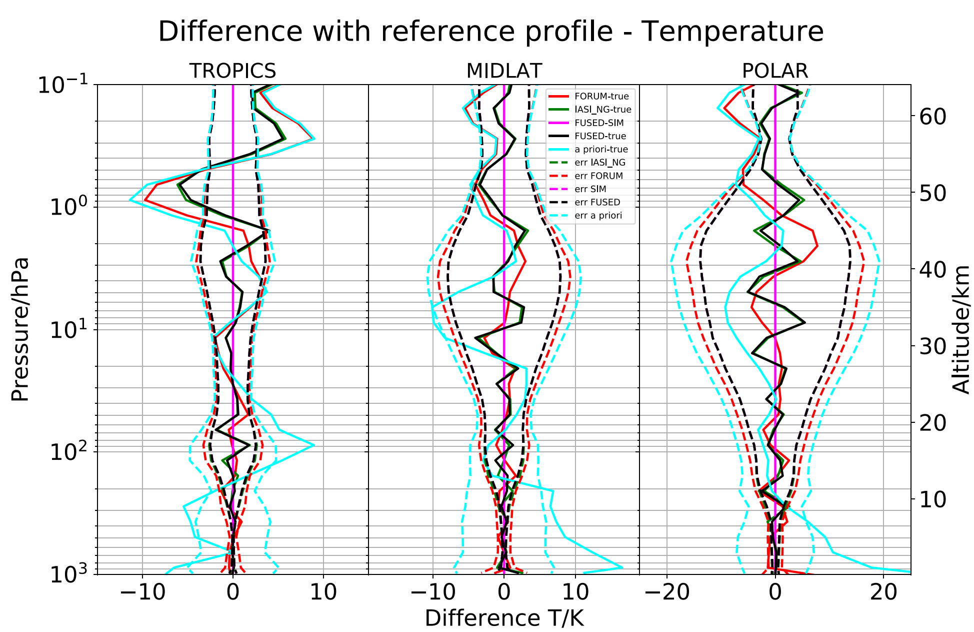

Fig. 4. Absolute differences between IASI-NG (green line), FORUM (red line), fused (black line), a priori (cyan line) profiles and the true profile for temperature in the three atmospheric scenarios: TROPICS (left), MIDLAT (central) and POLAR (right). Also shown are: the differences between the fused and the synergistic (SYN) profile (magenta line) and the total errors for all profiles (dashed lines, same colour coding of the profiles). The total errors of the synergistic and fused products are completely overlapped, thus it is impossible to distinguish the corresponding curves.

fused and the synergistic retrieval profiles is zero for all pressure levels as expected in the linear approximation case [14]. In this case the analysis of the comparison between the total errors (see Eq. (18) and (22)) of the fused (and synergistic) retrieval and mono-instrumental retrievals provides interesting information (see Fig. 4 and 5). The total errors for the fused profile are smaller or comparable to those of the individual products but some features, discussed in the following, are more significant.

Considering the temperature retrieval (Fig. 4), the FORUM total error is ~ 10% greater than that of the fused product in the altitude range from nearly 15 km up to the top of atmosphere, while it increases up to 70% in the lower layers. It is interesting to note that the differences between the total error of FORUM and fused retrievals decrease by 20% in the lower layers for the polar scenario, where FORUM retrievals are expected to be more informative [34]. The total errors of the IASI-NG temperature retrieval differ from those of the fused one by less than 0.1% from nearly 20 km up to the top of atmosphere while, near the surface differences increase up to ~ 3–4% from 0 to 7 km. The interesting behaviour is that from ~ 7 to 18 km the total error of IASI-NG is greater than

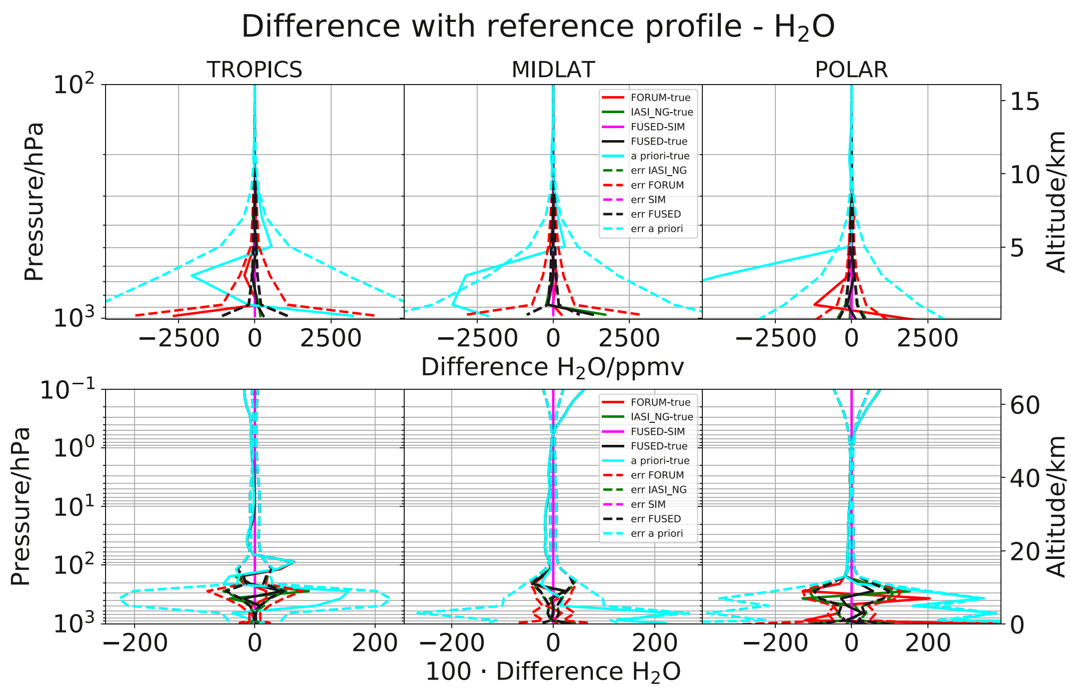

Fig. 5. Absolute (top) and percentage (bottom) differences between IASI-NG (green line), FORUM (red line), fused (black line), a priori (cyan line) profiles and the true profile for water vapour in the 3 atmospheric scenarios: TROPICS (left), MIDLAT (central) and POLAR (right). Also shown are: the differences between the fused and the synergistic (SYN) profile (magenta line) and the total errors for all profiles (dashed lines, same colour coding of the profiles). The total errors of the synergistic and fused products are completely overlapped, thus it is impossible to distinguish the corresponding curves.

that of the fused profile by the 10% (TROPICS) up to 21% (MIDLAT and POLAR), where FORUM contribution to the fused product is not negligible [33].

Considering the H_2O retrieval (Fig. 5), the reduction of the total error for the fused product with respect to FORUM is very high in the lower altitude layers up to 15 km, with values reaching 70–80 % in the TROPICS and MIDLAT scenarios. For these altitudes the IASI-NG total error is from 5 to 10% higher than that of the fused product for TROPICS and MIDLAT scenarios and higher than 10% for the polar atmosphere. On the contrary, in the lower layers of the polar atmosphere the FORUM total error is reduced by the 15–20% with respect to the other scenarios.

Resuming and considering all cases, differences of the fused profile with the true profile are smaller or comparable with the differences of individual measurements with the true profile and they are within the acceptable measuring range defined by the error statistics.

The number of DOFs and the SIC values are shown in Table 3 for all the retrieved profiles and all scenarios. The fused and synergistic profiles show the same number of DOFs, that is the greatest for all parameters and all scenarios with respect to the individual products: the mean values are 17.4 for temperature (from 15.5 for TROPICS to 18.7 for POLAR) and 6.7 for H_2O (from 6.2 for POLAR to 7.4 for TROPICS). For temperature the differences between the DOFs values of IASI-NG and fused (or synergistic retrieval) profile are less than 0.2 while for FORUM they vary from 4.4 (TROPICS) to 6.4 (POLAR). For H_2O differences between the DOFs of the individual measurements and the fused (or synergistic retrieval) products are less than 1.1. Concluding, the number of DOFs of the fused temperature retrievals are 1% larger with respect to IASI-NG and almost 45% with respect to FORUM while the number of DOFs for H_2O fused retrievals are 3% larger with respect to IASI-NG and almost 15% larger with respect to FORUM. The SIC values demonstrate the higher information content brought by the data fusion and the synergistic retrieval, confirming the results obtained for the DOFs analysis.

Table 3
Number of DOFs and SIC for IASI-NG, FORUM, fused and synergistic retrieval profiles for temperature and H_2O for the three scenarios: TROPICS, MIDLAT and POLAR.

		N. of DOFs - SIC [bit]	
Scenario	Profile	T	H_2O
TROPICS	IASI-NG	15.4 - 58.7	7.1 - 33.4
	FORUM	11.1 - 30.9	6.3 - 20.5
	FUSED	15.5 - 59.5	7.4 - 34.3
	SYNERGISTIC	15.5 - 59.5	7.4 - 34.3
MIDLAT	IASI-NG	17.6 - 67.3	6.3 - 28.9
	FORUM	12.4 - 37.8	5.6 - 18.0
	FUSED	17.8 - 68.7	6.4 - 29.5
	SYNERGISTIC	17.8 - 68.7	6.4 - 29.5
POLAR	IASI-NG	18.6 - 72.5	6.0 - 24.9
	FORUM	12.3 - 40.1	5.4 - 17.6
	FUSED	18.7 - 73.8	6.2 - 26.2
	SYNERGISTIC	18.7 - 73.8	6.2 - 26.2

For the first case of the study, Figs. 2 to 5 and the analysis of the number of DOFs demonstrate that the results of the CDF applied to IASI-NG and FORUM products and of the synergistic retrieval are equivalent also when the CDF algorithm is applied to MTRs (see Appendix in [14]). It is apparent that, when a parameter is retrieved by both IASI-NG and FORUM, the fused product obtaines most of the information content from IASI-NG but FORUM contribution is not negligible, in particular in the lower layers of the polar scenario and in the UTLS region.

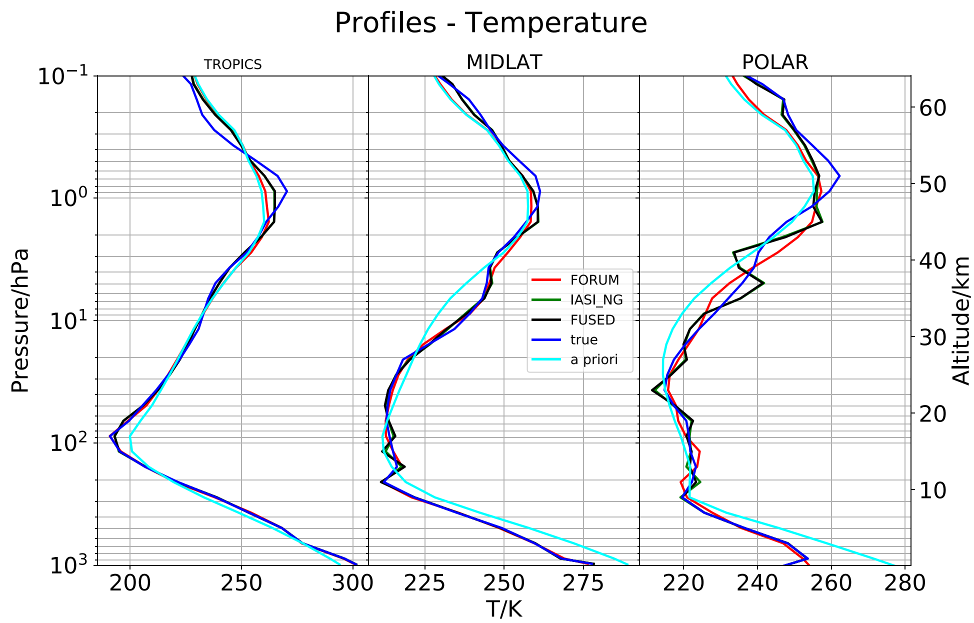

Fig. 6. Temperature profiles for IASI-NG (green line), FORUM (red line) and fused (black line) products and the corresponding true profile (blue line) in the three atmospheric scenarios: TROPICS (left), MIDLAT (central) and POLAR (right). The a priori profile is also shown (cyan line).

5.2. Experiment 2: MTR with different retrieved parameters

In this case, the state vectors of the fusing measurements IASI-NG and FORUM contain different atmospheric variables: temperature (T) is in common, water vapour (H_2O) is retrieved by FORUM and ozone (O_3) by IASI-NG. We applied the CDF algorithm using Eqs. (9), (11) and (12) that in this case become:

$$\hat{\mathbf{x}}_F = \begin{pmatrix} \mathbf{T}_F \\ \mathbf{H_2O}_F \\ \mathbf{0} \end{pmatrix} \mathbf{A}_F = \begin{pmatrix} \mathbf{A}_{\mathbf{T},F} & \mathbf{A}_{\mathbf{TH_2O},F} & 0 \\ \mathbf{A}_{\mathbf{H_2OT},F} & \mathbf{A}_{\mathbf{H_2O},F} & 0 \\ 0 & 0 & 0 \end{pmatrix} \quad \mathbf{S}_F = \begin{pmatrix} \mathbf{S}_{\mathbf{T},F} & \mathbf{S}_{\mathbf{TH_2O},F} & 0 \\ \mathbf{S}_{\mathbf{H_2OT},F} & \mathbf{S}_{\mathbf{H_2O},F} & 0 \\ 0 & 0 & 0 \end{pmatrix} \tag{26}$$

$$\hat{\mathbf{x}}_I = \begin{pmatrix} \mathbf{T}_I \\ \mathbf{0} \\ \mathbf{O_3}_I \end{pmatrix} \mathbf{A}_I = \begin{pmatrix} \mathbf{A}_{\mathbf{T},I} & 0 & \mathbf{A}_{\mathbf{TO_3},I} \\ 0 & 0 & 0 \\ \mathbf{A}_{\mathbf{O_3T},I} & 0 & \mathbf{A}_{\mathbf{O_3},I} \end{pmatrix} \mathbf{S}_I = \begin{pmatrix} \mathbf{S}_{\mathbf{T},I} & 0 & \mathbf{S}_{\mathbf{TO_3},I} \\ 0 & 0 & 0 \\ \mathbf{S}_{\mathbf{O_3T},I} & 0 & \mathbf{S}_{\mathbf{O_3},I} \end{pmatrix} \tag{27}$$

The fused state vector contains the three parameters temperature, H_2O and O_3:

$$\hat{\mathbf{x}}_f = \begin{pmatrix} \mathbf{T}_f \\ \mathbf{H_2O}_f \\ \mathbf{O_3}_f \end{pmatrix} \mathbf{A}_f = \begin{pmatrix} \mathbf{A}_{\mathbf{T},f} & \mathbf{A}_{\mathbf{TH_2O},f} & \mathbf{A}_{\mathbf{TO_3},f} \\ \mathbf{A}_{\mathbf{H_2OT},f} & \mathbf{A}_{\mathbf{H_2O},f} & \mathbf{A}_{\mathbf{H_2OO_3},f} \\ \mathbf{A}_{\mathbf{O_3T},f} & \mathbf{A}_{\mathbf{O_3H_2O},f} & \mathbf{A}_{\mathbf{O_3},f} \end{pmatrix} \quad \mathbf{S}_f = \begin{pmatrix} \mathbf{S}_{\mathbf{T},f} & \mathbf{S}_{\mathbf{TH_2O},f} & \mathbf{S}_{\mathbf{TO_3},f} \\ \mathbf{S}_{\mathbf{H_2OT},f} & \mathbf{S}_{\mathbf{H_2O},f} & \mathbf{S}_{\mathbf{H_2OO_3},f} \\ \mathbf{S}_{\mathbf{O_3T},f} & \mathbf{S}_{\mathbf{O_3H_2O},f} & \mathbf{S}_{\mathbf{O_3},f} \end{pmatrix} \tag{28}$$

The profiles of temperature, H_2O and O_3 are shown in Figs. 6, 7 and 8, respectively.

As in the previous case, the absolute differences between the individual (green line for IASI-NG, red line for FORUM), the fused (black line), the a priori (cyan line) and the true (blue line) profiles are calculated for temperature, H_2O and O_3 (Figs. 9, 10 and 11, respectively). The percentage differences (Eq. (16)) are calculated between FORUM and fused profiles and the true profile for H_2O (Fig. 10) and between IASI-NG and fused profiles and the true profile for O_3 (Fig. 11). In all cases the percentage differences between the a priori profile and the true profile are also calculated.

In this case, temperature is retrieved by both instruments as in the case of fusing vectors with two coinciding sets of variables thus, comments about profiles, differences and total errors are identical to those described above. H_2O here is retrieved only by FORUM and Fig. 10 shows high difference values in the troposphere (in particular, for the polar scenario) where the water vapour concentration is higher than 100 ppmv (see Fig. 7). The ozone profiles (Fig. 8) show a concentration peak between 30 and 40 km and differences between the profiles are higher below 20 km of altitude and around the peak, as reported by the analysis of absolute and percentage differences (Fig. 11).

In Table 4, the number of DOFs and Shannon Information Content (SIC) are shown for all the retrieved profiles and all scenarios. In all cases, the fused profile has the greatest number of DOFs: mean values are 17.3 (from 15.7 for TROPICS to 18.6 for POLAR) for temperature, 6.3 (from 5.7 for POLAR to 7.0 for TROPICS) for H_2O and 3.8 (from 2.9 for POLAR to 4.4 for TROPICS) for O_3. Considering the number of DOFs for temperature, the differences between fused and IASI-NG profiles are smaller than 0.2, while for FORUM vary between 4.6 (TROPICS) and 6.3 (POLAR). For water vapour, in this case retrieved only by FORUM, the differences with fused values are less than 1.3 for all scenarios while for ozone, retrieved by IASI-NG only, are 0.01 for all scenarios.

Also in this case, it is apparent that, when a parameter is retrieved by both IASI-NG and FORUM, the fused product obtains most of the information content from IASI-NG. Moreover, the fact that the fused product has a greater value of number of DOFs for the parameters that are not in common is an evidence of the improvement guaranteed by applying the CDF: more information on the parameter in common provides more information also on the one not in common. If we analyse Figs. 7, 10 and Table 4 for H_2O it is evident that, even if the water vapour profile is measured only by FORUM, the fused profile shows a significantly smaller error and smaller difference values with the true profile and a grater number of DOFs with respect to the FORUM profile.

The results obtained about the number of DOFs for the temperature retrievals (the common parameter) are equivalent, as expected, to those obtained in the first case. If we consider the parameters not in common, we find that the number of DOFs of the H_2O retrieval (measured only by FORUM, in this case) is from 5%

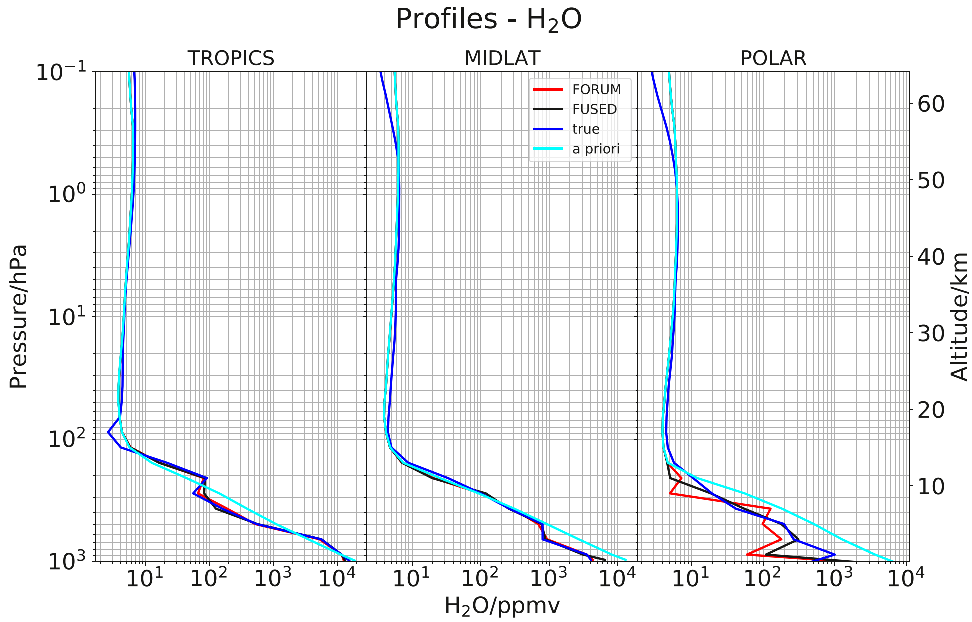

Fig. 7. Water vapour profiles for FORUM (red line) and fused (black line) products and the corresponding true profile (blue line) in the three atmospheric scenarios: TROPICS (left), MIDLAT (central) and POLAR (right). The a priori profile is also shown (cyan line).

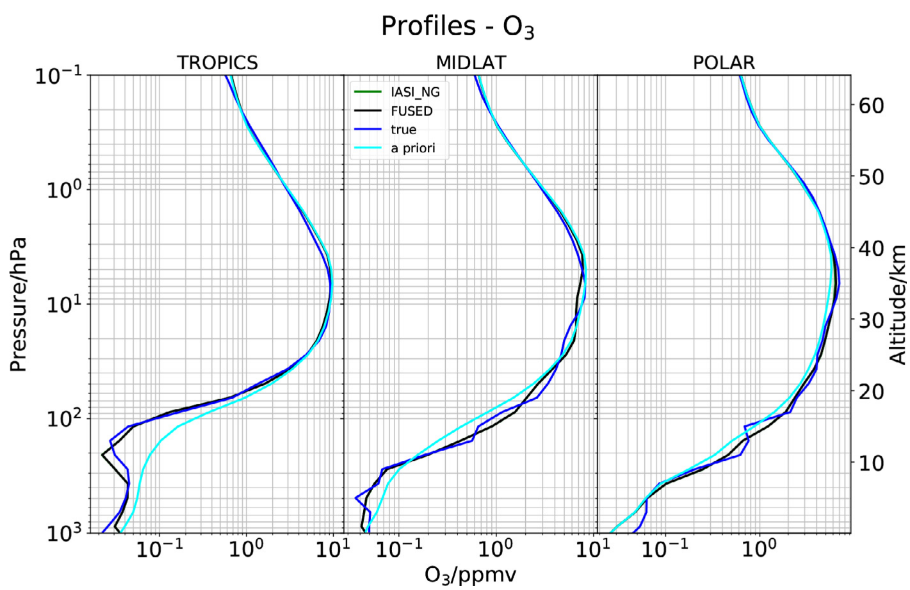

Fig. 8. Ozone profiles for IASI-NG (green line) and fused (black line) products and the corresponding true profile (blue line) in the three atmospheric scenarios: TROPICS (left), MIDLAT (central) and POLAR (right). The a priori profile is also shown (cyan line).

Table 4
Number of DOFs and SIC for IASI-NG, FORUM and fused profiles for temperature, H_2O and O_3 for the three atmospheric scenarios: TROPICS, MIDLAT and POLAR.

		N. of DOFs - SIC [bit]		
Scenario	Profile	T	H_2O	O_3
TROPICS	IASI-NG	15.6 - 69.4	/	4.4 - 14.2
	FORUM	11.1 - 30.9	6.3 - 20.5	/
	FUSED	15.7 - 70.0	7.0 - 32.2	4.4 - 14.2
MIDLAT	IASI-NG	17.5 - 76.4	/	4.1 - 11.4
	FORUM	12.4 - 37.8	5.6 - 18.0	/
	FUSED	17.7 - 77.3	6.1 - 28.7	4.1 - 11.5
POLAR	IASI-NG	18.5 - 79.5	/	2.9 - 6.2
	FORUM	12.3 - 40.1	5.4 - 17.6	/
	FUSED	18.6 - 80.2	5.7 - 25.6	2.9 - 6.3

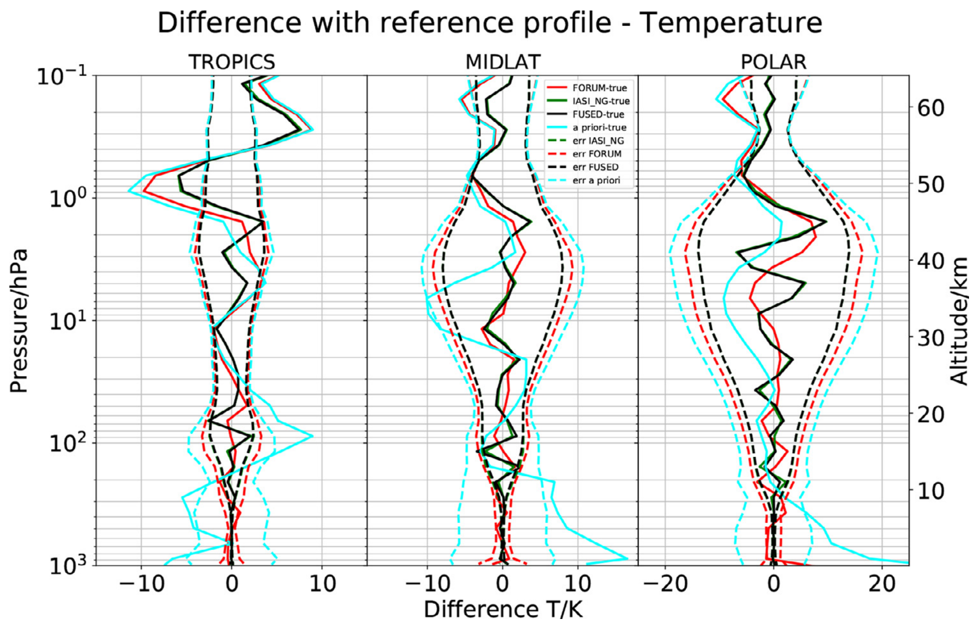

Fig. 9. Absolute differences between IASI-NG (green line), FORUM (red line), fused (black line), a priori (cyan line) profiles and the true profile for temperature in the three atmospheric scenarios: TROPICS (left), MIDLAT (central) and POLAR (right). The total errors are also shown for all profiles (dashed lines, same colour coding of the profiles).

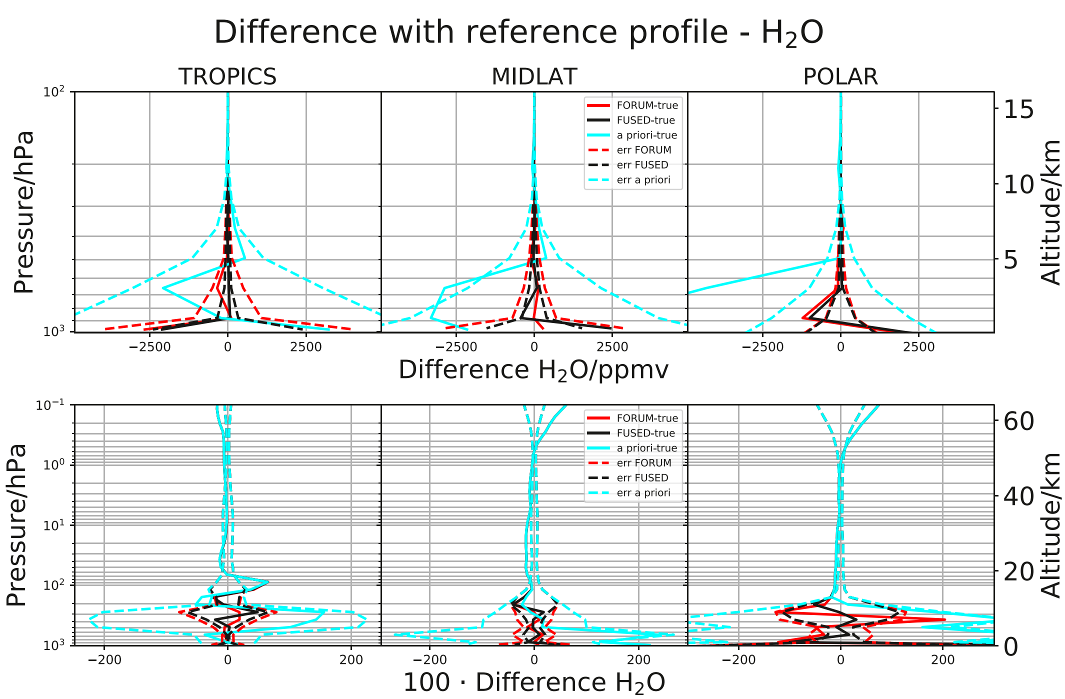

Fig. 10. Absolute (top) and percentage (bottom) differences between FORUM (red line), fused (black line), a priori (cyan line) profiles and the true profile for water vapour in the three atmospheric scenarios: TROPICS (left), MIDLAT (central) and POLAR (right). The total errors are also shown for all profiles (dashed lines, same colour coding of the profiles).

(POLAR) to almost 11% (TROPICS) larger for the fused product. The increase in the number of DOFs for the O_3 retrieval (measured only by IASI-NG, in this case) is very small: almost 0.2%. The values obtained for the SIC confirmed the results of the DOFs analysis showing an information gain of the fused product enhanced of almost 50% for temperature, over 30% for H_2O and less than 0.6% for O_3. These results demonstrate that the application of the CDF procedure to MTR products with one parameter in common and a subset of mono-instrumental retrieved parameters, provides a gain in the retrieval information content both for the parameter in common and for the not in common ones. Moreover, this gain is directly connected to the correlation between the parameter in common (temperature in this case) and the mono-instrumental ones (O_3 and H_2O in this case): the higher is the correlation, the higher

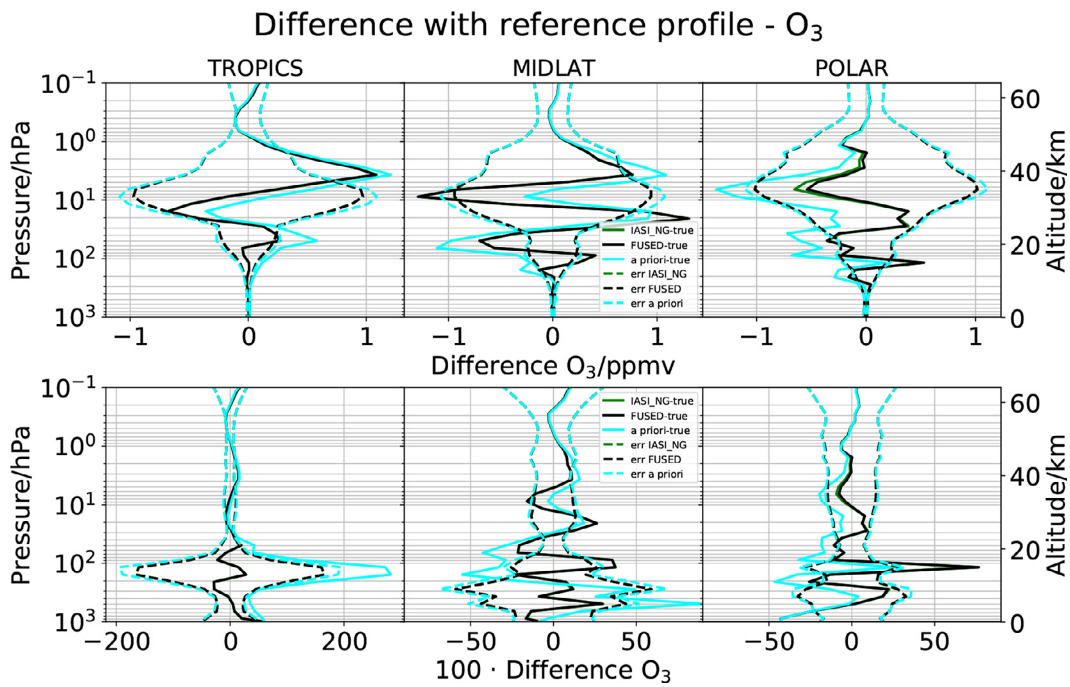

Fig. 11. Absolute (top) and percentage (bottom) differences between IASI-NG (green line), fused (black line), a priori (cyan line) profiles and the true profile for ozone in the three atmospheric scenarios: TROPICS (left), MIDLAT (central) and POLAR (right). The total errors are also shown for all profiles (dashed lines, same colour coding of the profiles).

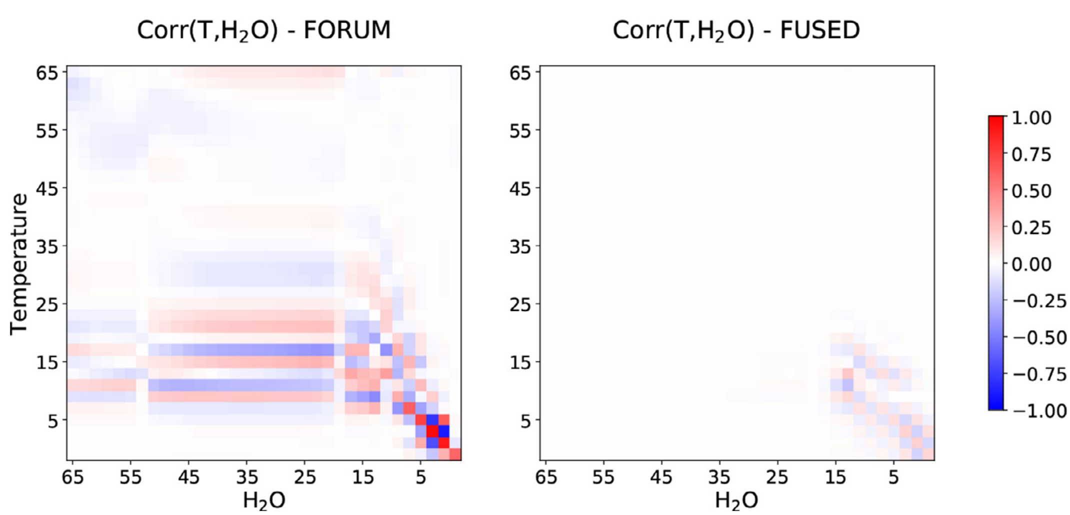

Fig. 12. Correlations among the retrieved atmospheric profiles of experiment 2: temperature and H_2O. Left: FORUM; right: fused product. The maps scale is shown in km of altitude.

is the information gain. Looking to our specific case: temperature and H_2O are highly correlated, thus the consistent improvement in the number of DOFs for the fused temperature retrieval with respect to FORUM (45%) guarantees a gain in the fused H_2O retrieval of the 7–8% with respect to the mono-instrumental retrieval of FORUM. The correlation between temperature and O_3 is weaker, consequently the CDF application effect for the O_3 retrieval is significantly smaller. The correlations between the profiles of the retrieved parameters are visualized in Figs. 12 and 13 where we show the correlation matrices limited to the submatrices relative to the correlations between the profiles of T and H_2O for FORUM and the fused product and between T and O_3 for IASI-NG and the fused product. For the individual instruments vertical correlations are stronger between the profiles of temperature and water vapour in particular for the atmospheric layers below 10 km. The correlation between temperature and ozone is weaker and limited to the lower stratosphere. Comparing the results obtained for individual retrievals with those obtained for the fused product, it is evident that the CDF application strongly reduces the correlations between temperature and H_2O and almost sets to zero the correlations between temperature and O_3.

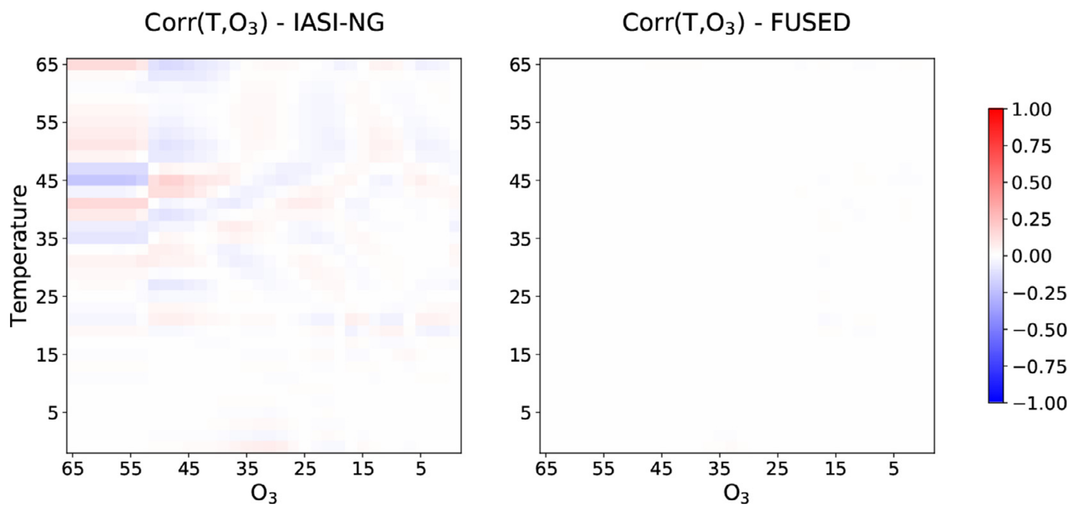

Fig. 13. Correlations among the retrieved atmospheric profiles of experiment 2: temperature and O_3. Left: IASI-NG; right: fused product. The maps scale is shown in km of altitude.

6. Conclusions

In this work, we described how to extend the use of the CDF algorithm to MTR products and demonstrated its first application to simulated retrievals of IASI-NG and FORUM, as their measurements will be suitable for synergistic approaches. We analysed simulated retrievals of temperature, H_2O and O_3 in two experiments: in experiment 1, the state vectors from MTRs include the same variables, in experiment 2 they share only a subset of variables. As first test, we considered three different atmospheric scenarios (TROPICS, MIDLAT and POLAR), we simulated the FORUM and IASI-NG profiles as exactly co-located (in space and time) and defined on the same vertical grid. The same a priori profile is considered for the simulated retrievals. In both experiments, all the retrieval products are simulated adopting the linear approximation.

In the analysis of the results, we demonstrated the capability of the generalized CDF to deal with different state vectors, assuring outputs of improved quality with respect to the input data. In both experiments, the total errors of the fused profile are smaller or comparable with those of the individual products, the number of DOFs and the SIC values of the fused profile are greater than those of the IASI-NG and FORUM products, demonstrating that the fused profile guarantees the greatest amount of information compared to the individual products.

In experiment 1 we showed the equivalence of the two synergistic approaches also when the CDF algorithm is applied to MTR products, simulated in linear approximation. Through experiment 2 we demonstrated that the CDF also improves the parameters that are observed only by one of the instruments. Moreover, we showed that the gain in the information content for the parameters not in common is directly connected to the level of correlation between the parameter in common and those not in common.

As MTRs are increasingly applied to the analysis of remote sensing observations for their capability to simultaneously retrieve multiple variables with an high accuracy, the generalization of the CDF to MTR products is a crucial achievement in order to extend its application to a greater number of high-value remote sensing data. The results obtained demonstrate, within the approximations adopted in this case study, a comparable or better quality of the fused products with respect to that of the individual products of MTRs in all the considered cases.

Funding

This research was carried out in the framework of the project OT4CLIMA which was funded by the Italian Ministry of Education, University and Research (D.D. 2261 del 6.9.2018, PON R&I 2014-2020 and FSC).

Declaration of Competing Interest

The authors declare that they have no known competing financial interests or personal relationships that could have appeared to influence the work reported in this paper.

References

[1] Lahoz WA, Geer AJ, Bekki S, Bormann N, Ceccherini S, Elbern H, et al. The assimilation of envisat data (ASSET) project. Atmos Chem Phys 2007;7(7):1773–96. doi:10.5194/acp-7-1773-2007.

[2] Clarisse L, R'Honi Y, Coheur P-F, Hurtmans D, Clerbaux C. Thermal infrared nadir observations of 24 atmospheric gases. Geophys Res Lett 2011;38(10). doi:10.1029/2011GL047271.

[3] Fischer H, Birk M, Blom C, Carli B, Carlotti M, von Clarmann T, et al. MIPAS: an instrument for atmospheric and climate research. Atmos Chem Phys 2008;8(8):2151–88. doi:10.5194/acp-8-2151-2008.

[4] Bovensmann H, Burrows JP, Buchwitz M, Frerick J, Nol S, Rozanov VV, et al. SCIAMACHY: mission objectives and measurement modes. J Atmos Sci 1999;56(2):127–50. doi:10.1175/1520-0469(1999)056<0127:SMOAMM>2.0.CO;2.

[5] Bernath PF, McElroy CT, Abrams MC, Boone CD, Butler M, Camy-Peyret C, et al. Atmospheric chemistry experiment (ACE): mission overview. Geophys Res Lett 2005;32(15). doi:10.1029/2005GL022386.

[6] Waters J, Froidevaux L, Harwood R, Jarnot R, Pickett H, Read W, et al. The earth observing system microwave limb sounder (EOS MLS) on the aura satellite. IEEE Trans Geosci Remote Sens 2006;44(5):1075–92. doi:10.1109/TGRS.2006.873771.

[7] Aires F, Aznay O, Prigent C, Paul M, Bernardo F. Synergistic multi-wavelength remote sensing versus a posteriori combination of retrieved products: application for the retrieval of atmospheric profiles using metop-A. J Geophys Res 2012;117(D18). doi:10.1029/2011JD017188.

[8] Cuesta J, Eremenko M, Liu X, Dufour G, Cai Z, Höpfner M, et al. Satellite observation of lowermost tropospheric ozone by multispectral synergism of IASI thermal infrared and GOME-2 ultraviolet measurements over Europe. Atmos Chem Phys 2013;13(19):9675–93. doi:10.5194/acp-13-9675-2013.

[9] Costantino L, Cuesta J, Emili E, Coman A, Foret G, Dufour G, et al. Potential of multispectral synergism for observing ozone pollution by combining IASI-NG and UVNS measurements from the EPS-SG satellite. Atmos Meas Tech 2017;10(4):1281–98. doi:10.5194/amt-10-1281-2017.

[10] Cortesi U, Ceccherini S, Del Bianco S, Gai M, Tirelli C, Zoppetti N, et al. Advanced ultraviolet radiation and ozone retrieval for applications (AURORA): a project overview. Atmosphere 2018;9(11). doi:10.3390/atmos9110454.

[11] Sato TO, Sato TM, Sagawa H, Noguchi K, Saitoh N, Irie H, et al. Vertical profile of tropospheric ozone derived from synergetic retrieval using three different wavelength ranges, UV, IR, and microwave: sensitivity study for satellite observation. Atmos Meas Tech 2018;11(3):1653–68. doi:10.5194/amt-11-1653-2018.
[12] Fu D, Worden JR, Liu X, Kulawik SS, Bowman KW, Natraj V. Characterization of ozone profiles derived from Aura TES and OMI radiances. Atmos Chem Phys 2013;13(6):3445–62. doi:10.5194/acp-13-3445-2013.
[13] Aires F. Measure and exploitation of multisensor and multiwavelength synergy for remote sensing: 1. Theoretical considerations. J Geophys Res 2011;116(D2). doi:10.1029/2010JD014701.
[14] Ceccherini S, Carli B, Raspollini P. Equivalence of data fusion and simultaneous retrieval. Opt Express 2015;23(7):8476–88. doi:10.1364/OE.23.008476.
[15] Warner JX, Yang R, Wei Z, Carminati F, Tangborn A, Sun Z, et al. Global carbon monoxide products from combined AIRS, TES and MLS measurements on a-train satellites. Atmos Chem Phys 2014;14(1):103–14. doi:10.5194/acp-14-103-2014.
[16] Schneider M, Ertl B, Diekmann CJ, Khosrawi F, Weber A, Hase F, et al. Design and description of the MUSICA IASI full retrieval product. Earth Syst Sci Data Discuss 2021;2021:1–51. doi:10.5194/essd-2021-75.
[17] Ceccherini S, Carli B, Tirelli C, Zoppetti N, Del Bianco S, Cortesi U, et al. Importance of interpolation and coincidence errors in data fusion. Atmos Meas Tech 2018;11(2):1009–17. doi:10.5194/amt-11-1009-2018.
[18] Tirelli C, Ceccherini S, Zoppetti N, Del Bianco S, Gai M, Barbara F, et al. Data fusion analysis of sentinel-4 and sentinel-5 simulated ozone data. J Atmos Oceanic Technol 2020;37(4):573–87. doi:10.1175/JTECH-D-19-0063.1.
[19] Zoppetti N, Ceccherini S, Carli B, Del Bianco S, Gai M, Tirelli C, et al. The complete data fusion for a full exploitation of copernicus atmospheric sentinel level 2 products. Atmos Meas Tech Discuss 2019;2019:1–13. doi:10.5194/amt-2019-436.
[20] Dinelli B, Alpaslan D, Carlotti M, Magnani L, Ridolfi M. Multi-target retrieval (MTR): the simultaneous retrieval of pressure, temperature and volume mixing ratio profiles from limb-scanning atmospheric measurements. J Quant Spectrosc Radiat Transfer 2004;84(2):141–57. doi:10.1016/S0022-4073(03)00137-7.
[21] Dinelli BM, Arnone E, Brizzi G, Carlotti M, Castelli E, Magnani L, et al. The MIPAS2D database of MIPAS/ENVISAT measurements retrieved with a multi-target 2-dimensional tomographic approach. Atmos Meas Tech 2010;3(2):355–74. doi:10.5194/amt-3-355-2010.
[22] Carlotti M, Brizzi G, Papandrea E, Prevedelli M, Ridolfi M, Dinelli BM, et al. GMTR: two-dimensional geo-fit multitarget retrieval model for michelson interferometer for passive atmospheric sounding/environmental satellite observations. Appl Opt 2006;45(4):716–27. doi:10.1364/AO.45.000716.
[23] Papandrea E, Arnone E, Brizzi G, Carlotti M, Castelli E, Dinelli BM, et al. Two-dimensional tomographic retrieval of MIPAS/ENVISAT measurements of ozone and related species. Int J Remote Sens 2010;31(2):477–83. doi:10.1080/01431160902893501.
[24] Clerbaux C, Boynard A, Clarisse L, George M, Hadji-Lazaro J, Herbin H, et al. Monitoring of atmospheric composition using the thermal infrared IASI/MetOp sounder. Atmos Chem Phys 2009;9(16):6041–54. doi:10.5194/acp-9-6041-2009.
[25] Hilton F, Armante R, August T, Barnet C, Bouchard A, Camy-Peyret C, et al. Hyperspectral earth observation from IASI: five years of accomplishments. Bull Am Meteorol Soc 2012;93(3):347–70. doi:10.1175/BAMS-D-11-00027.1.
[26] Crevoisier C, Clerbaux C, Guidard V, Phulpin T, Armante R, Barret B, et al. Towards IASI-New generation (IASI-NG): impact of improved spectral resolution and radiometric noise on the retrieval of thermodynamic, chemistry and climate variables. Atmos Meas Tech 2014;7:4367–85. doi:10.5194/amt-7-4367-2014.
[27] Crevoisier C., Clerbaux C., Guidard V., Phulpin T., Armante R., Barret B., et al. The IASI-NG mission onboard METOP-SG: scientific objectives and expected results 2013; URL https://hal.archives-ouvertes.fr/hal-01004672.
[28] Rodgers C.D., et al. Inverse methods for atmospheric sounding: theory and practice. 2000.
[29] Ceccherini S, Carli B, Pascale E, Prosperi M, Raspollini P, Dinelli BM. Comparison of measurements made with two different instruments of the same atmospheric vertical profile. Appl Opt 2003;42(32):6465–73. doi:10.1364/AO.42.006465.
[30] Ceccherini S, Ridolfi M. Technical note: variance-covariance matrix and averaging kernels for the Levenberg-Marquardt solution of the retrieval of atmospheric vertical profiles. Atmos Chem Phys 2010;10(6):3131–9. doi:10.5194/acp-10-3131-2010.
[31] Ceccherini S, Carli B, Raspollini P. Vertical grid of retrieved atmospheric profiles. J Quant Spectrosc Radiat Transfer 2016;174:7–13. doi:10.1016/j.jqsrt.2016.01.018.
[32] Kalman R. Algebraic aspects of the generalized inverse of a rectangular matrix. In: Generalized inverses and applications. Elsevier; 1976. p. 111–24. doi:10.1016/b978-0-12-514250-2.50006-8.
[33] Ridolfi M, Del Bianco S, Di Roma A, Castelli E, Belotti C, Dandini P, et al. Forum earth explorer 9: characteristics of level 2 products and synergies with IASI-NG. Remote Sens 2020;12(9). doi:10.3390/rs12091496.
[34] Palchetti L, Brindley H, Bantges R, Buehler SA, Camy-Peyret C, Carli B, et al. FORUM: unique far-infrared satellite observations to better understand how Earth radiates energy to space. Bull Am Meteorol Soc 2020:1–52. doi:10.1175/BAMS-D-19-0322.1.
[35] EUMETSAT. EPS-SG IASI-NG2021Accessed: 2021-01-25, URL https://www.eumetsat.int/eps-sg-iasi-ng.
[36] Cortesi U, Del Bianco S, Gai M, Laurenza LM, Ceccherini S, Carli B, et al. Sensitivity analysis and application of KLIMA algorithm to GOSAT and OCO validation. Tech Sci Res Rep 2014;6:1–153.
[37] Lacour J-L, Risi C, Clarisse L, Bony S, Hurtmans D, Clerbaux C, et al. Mid-tropospheric δd observations from IASI/MetOp at high spatial and temporal resolution. Atmos Chem Phys 2012;12(22):10817–32. doi:10.5194/acp-12-10817-2012.
[38] Worden J, Bowman K, Noone D, Beer R, Clough S, Eldering A, et al. Tropospheric emission spectrometer observations of the tropospheric HDO/H2O ratio: estimation approach and characterization. J Geophys Res 2006;111(D16). doi:10.1029/2005JD006606.
[39] Herbin H, Hurtmans D, Clerbaux C, Clarisse L, Coheur P-F. $H_2{}^{16}O$ and HDO measurements with IASI/MetOp. Atmos Chem Phys 2009;9(24):9433–47. doi:10.5194/acp-9-9433-2009.
[40] Gelaro R, McCarty W, Surez MJ, Todling R, Molod A, Takacs L, et al. The modern-era retrospective analysis for research and applications, version 2 (MERRA-2). J Clim 2017;30(14):5419–54. doi:10.1175/JCLI-D-16-0758.1.
[41] Remedios JJ, Leigh RJ, Waterfall AM, Moore DP, Sembhi H, Parkes I, et al. MIPAS reference atmospheres and comparisons to v4.61/v4.62 MIPAS level 2 geophysical data sets. Atmos Chem Phys Discuss 2007;7:9973–10017. doi:10.5194/acpd-7-9973-2007.
[42] Liuzzi G, Masiello G, Serio C, Venafra S, Camy-Peyret C. Physical inversion of the full IASI spectra: assessment of atmospheric parameters retrievals, consistency of spectroscopy and forward modelling. J Quant Spectrosc Radiat Transf 2016;182:128–57. doi:10.1016/j.jqsrt.2016.05.022.
[43] ECMWF. MARS2021; Accessed: 2020-11-09, URL https://confluence.ecmwf.int/display/UDOC/MARS+user+documentation.
[44] Zoppetti N, Ceccherini S, Carli B, Del Bianco S, Gai M, Tirelli C, et al. Application of the complete data fusion algorithm to the ozone profiles measured by geostationary and low-earth-orbit satellites: a feasibility study. Atmos Meas Tech 2021;14(3):2041–53. doi:10.5194/amt-14-2041-2021.